doi:10.14311/ppt.2019.2.119
Plasma Physics and Technology **6**(2):119–122, 2019

INFLUENCE OF RESONANCE RADIATION TRANSPORT ON CHEMICAL EQUILIBRIUM IN AN ARGON ARC

S. Gortschakow[a,*], D. Kalanov[b], Yu. Golubovskii[c]

[a] *Leibniz Institute for Plasma Science and Technology (INP), Felix-Hausdorff-Strasse 2, 17489 Greifswald, Germany*

[b] *Leibniz Institute of Surface Engineering (IOM), Permoserstrasse 15, 04318 Leipzig, Germany*

[c] *Saint-Petersburg State University, Ulyanovskaya 3, 198504 St. Petersburg, Russia*

[*] sergey.gortschakow@inp-greifswald.de

Abstract. Deviations from chemical equilibrium in argon arc plasma are analysed by means of collisional-radiative model. Corresponding comprehensive kinetic scheme has been developed and applied form study of free-burning arc at the conditions typical for welding applications. While the natural lifetime have been used for radiation emitted from highly excited argon states, the resonance radiation was described taking into account the radiation transport effects. Resulting spatial distributions of excited argon atoms are compared for the cases of LTE and two-temperature plasma using different approaches for the description of the resonance radiation transport.

Keywords: radiation transport, collisional-radiative model, argon arc.

1. Introduction

Modern arc simulations take into account the deviations from equilibrium plasma state in order to reach a better agreement with experiments. In addition to thermal non-equilibrium the departures from chemical equilibrium are of specific interest since they are essential for plasma properties in the colder regions. In general, the description of plasma chemistry requires application of collisional-radiative models. In recent papers devoted to studies of the free-burning Ar arc [1–3] a self-consistent two-temperature fluid model with accounting for non-equilibrium effects was presented. The modelling approach is based on the solution of the Navier-Stokes equations for mass, energy, and momentum conservation along with the equations of electric continuity, Ohm's and Ampere's law, which self-consistently determine electric and self-induced magnetic plasma fields. Furthermore, the model comprises of the balance equations for different species, taking into account transport processes due to diffusion and convection, and various collisional-radiative transitions. The inclusion of radiation transport equations in the balance equations for individual particles in the frames of such description is a very challenging task. Therefore, the models [1–3] use effective lifetime approximation in order to take into account the corresponding radiation trapping. In the work [4], which used the input data from model [2], a matrix method for description of resonance radiation transport was proposed. Transport of resonance radiation is a notable process, which influences the formation of various spatially-temporal structures in the gas-discharge plasma. This type of the plasma transport competes with other transport mechanisms, such as diffusion and convection. Therefore, a correct consideration of the radiation trapping is an important point in plasma modelling.

In the present contribution the results obtained by collisional-radiative model with extended kinetic scheme are presented. As an extension of approach [4], the radiation transport accounts for all resonance states of argon atom, also several additional highly-excited levels have been taken into account. Furthermore, the model includes both the axial and radial dependency for the conditions typical for tungsten inert gas welding (TIG). Input parameters, such as gas and electron temperature profiles, electron density are predicted by a full non-equilibrium MHD model of TIG arc. Spatial distributions of excited atoms densities are compared with Boltzmann distribution, which characterizes the equilibrium plasma state. The contributions of collisional processes, radiative processes as well as of radiation transport for these regions are analysed with focus on deviations from equilibrium state.

2. Description of the model

Analysis of the deviations from equilibrium plasma state was performed through the comparison between three different models. Model A assumes that the chemical equilibrium state holds in the arc plasma and in the arc fringes, while models B and C use a comprehensive kinetic scheme for the determination of spatial profiles of species densities. The difference between the model B and model C arises from the different consideration of transport effects. Model B uses a widely applied approach of effective lifetime, i.e. the effect of radiation transport is summarized in prolonged lifetime of corresponding excited level, which is constant for all spatial positions. In contrast

to this, model C included the precise consideration of radiation transport process, which is space-dependent.

The collisional-radiative model use several input parameters determined by MHD model from [2, 3]. In present contribution the electron and gas temperature, as well as of the electron density obtained from the simulations of a TIG arc in argon are used.

2.1. LTE plasma

The majority of the arc models assumes that the plasma is in LTE state. First improvement of plasma description is provided by so-called two-temperature (2T) models. The two-temperature approach considers a separate energy balances for the electrons and heavy particles. However, the 2T approach still assumes that the distribution over excited levels follows the equilibrium rules. The chemical equilibrium in 2T plasma is determined by the electron temperature T_e and is described by Boltzmann distribution

$$\frac{N^*}{N_0} = \frac{g^*}{g_0} \mathrm{e}^{-\frac{E^*}{k_\mathrm{B} T_\mathrm{e}}} \tag{1}$$

where N^* and N_0 are the densities of excited and ground state, g^* and g_0 are the corresponding statistical weights and E^* is the excitation threshold of corresponding excited level.

The ion density n_i (and, therefore, due to the assumption of quasi-neutrality and presence of single-charged ions only, the electron density) can be determined from Saha equilibrium relation

$$n_i^2 = \frac{2}{\Lambda^3} \frac{Z_i}{Z_0} N_0 \mathrm{e}^{-\frac{E_{io}}{k_\mathrm{B} T_\mathrm{e}}} \tag{2}$$

with Debye length Λ, partition functions Z_0, Z_i and ionization energy E_{io}.

2.2. Collisional-radiative model

Collisional-radiative model takes into account the plasma-chemical processes in a free-burning argon arc using a 24 level model for argon. The included levels are: the ground state $1p_0$, metastable levels $1s_5$ and $1s_3$, resonance levels $1s_4$ and $1s_2$, individual radiating levels $2p_{10} - 2p_1$, lumped levels $3d$, $5s$, $5p$, $4d+6s$, $4f$, $6p$, $5d+7s$, $5f+5g$, as well as the ion in the ground state. Figure 1 shows the major plasma-chemical processes considered in the model. The kinetic scheme includes 611 plasma-chemical processes, among others excitation and de-excitation electron-atom collisions, collisional and photo-ionization, recombination, as well as various radiative processes. Corresponding data for reaction rates can be found in [2, 3]. While the natural lifetime has been used for radiation emitted from highly excited argon states the resonance radiation was described taking into account the radiation transport effects. For other radiation processes the plasma has been assumed to be optically thin and spontaneous transition probabilities were applied to calculate the radiation losses. The diffusive and

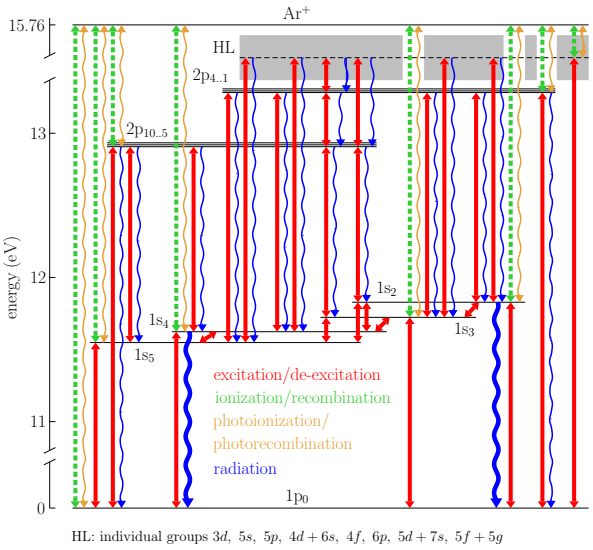

Figure 1. Argon kinetic scheme used in the model.

convective transport was neglected since the frequencies of the collisional-radiative processes are dominant at considered conditions. The balance equation for resonance states Ar($1s_4$,$1s_2$), (Holstein-Biberman equation) in the case of stationary plasma reads

$$\begin{aligned} A N_\mathrm{r}(\vec{r}) - A \int_V N_\mathrm{r}(\vec{r}) K(\vec{r}, \vec{r'}) \mathrm{d}^3 r' = \\ Z_\mathrm{r}^+(\vec{r}) - Z_\mathrm{r}^-(\vec{r}) + W_\mathrm{r}(\vec{r}). \end{aligned} \tag{3}$$

Here A is a spontaneous emission probability, N_r is the density of the resonance atoms, Z_r^- is total de-excitation per unit of time at the unit volume, Z_r^+ is the total excitation due to transitions from other states of considered system, W_r is a summary excitation due to transitions from ground state and recombination. The kernel of radiation transport operator $K(\vec{r}, \vec{r'})$ is the probability for a photon emitted in the point $\vec{r}$ to be absorbed in the point $\vec{r'}$. Considering spatial inhomogeneity of the absorption coefficient the kernel can be represented in the form

$$K(\vec{r}, \vec{r}') = \frac{1}{4\pi} \int_0^\infty \mathrm{d}\nu \frac{\epsilon_\nu(\vec{r}') \kappa_\nu(\vec{r})}{|\vec{r} - \vec{r}'|^2} e^{-\int_{\vec{r}'}^{\vec{r}} \kappa_\nu(\xi) \mathrm{d}\xi}, \tag{4}$$

where $\epsilon_\nu(\vec{r}')$ and $\kappa_\nu(\vec{r})$ are the line profiles of emission and absorption, and ν is the photon frequency. The expression under the integral describes the probability of the photon travel between the points $\vec{r}$ and $\vec{r}'$ without being absorbed.

The matrix solution approach [4] consists of discretization of the integral equation (3) by dividing the entire plasma volume into a number of small cells (n) in accordance with the chosen geometry. The discretization procedure is similar to that described in detail in the previous work [4]. In addition the axial dependency was taken into account by consideration

of finite number of axial positions. After discretization the left side of equation (3) at the position r_k takes the representation

$$AN_{\mathrm{r}}(\vec{r}) - A\int_V N_{\mathrm{r}}(\vec{r})K(\vec{r},\vec{r}')\mathrm{d}^3r' = \sum_{i=0}^{n-1} A_{\mathrm{eff}}N_{\mathrm{r}}(r_i)b_{i,k} \tag{5}$$

Here $b_{i,k}$ denotes the transport matrix and A_{eff} is the effective probability of radiative transition by Biberman [5, 6]. Finally, the equation system at the position r_k takes the following form

$$\sum_{q\neq m}\sum_{i=0}^{n} N_m(r_i)\left[A_{\mathrm{eff}}b_{k,i}\delta_{m=\mathrm{res},q} + Z^-_{m,q}(r_i)\right] = W_m(r_k) + \sum_{q\neq m} Z^+_{q,m}(r_k) \tag{6}$$

Here Z^+, Z^- denote the rates of excitations and de-excitations due to collisional-radiative transitions from states with index q, to state with index m. Kronecker delta $\delta(m = \mathrm{res}, q)$ allows for to formalize the equation for the case of radiation transport inclusion, e.g. in considered case the resonance radiation trapping process, relating to the $\mathrm{Ar}(1s_4)$ or $\mathrm{Ar}(1s_2)$ state. Notice, that in case of non-resonant atoms the radiation transport matrix reduces to an unit matrix and $A_{\mathrm{eff}} \equiv A$. Furthermore, in the case of non-radiating levels, like e.g. metastable, only the second term in the parenthesis in the left part of equation (6) remains.

Two different approaches have been used, namely effective lifetime approximation (model B, matrix $b_{i,k}$ is replaced by unity matrix) and solution of radiation transport equation by the matrix method (model C).

3. Results and discussion

Schematic view of the arc temperature distribution is given in Fig. 2. The input parameters correspond to following experimental conditions: arc length 8 mm, arc current 200 A DC, argon at atmospheric pressure between a conical tungsten cathode and a water cooled flat copper anode. Gas is fed through a nozzle near the cathode with a flow rate 12 slpm [1].

The results will be presented on example of excited levels $1s_4$, $2p_{10}$ and $2p_1$ (Fig. 3). Analysis has been done for the case with homogeneous absorption coefficient (k =1), since the spatial dependency of the absorption coefficient has much lower impact on the results in comparison with transport effects [4]. Determination of the density was performed for regions separated from electrodes by a distance of 1 mm in order to exclude the processes in the cathode and the anode layers where the application of the model is restricted. Figure 3 clarifies that the density profiles becomes more narrow for the states with higher excitation energy for all models. Introduction of radiation transport causes significant changes in the density

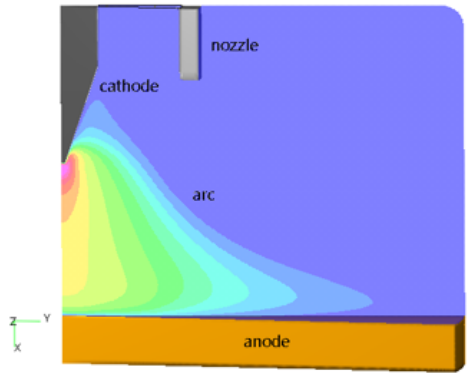

Figure 2. Schematic view of temperature distribution in a TIG arc.

distributions (cf. results from model A vs models B and C). (i) The radial profiles becomes much broader. (ii) Close to the cathode, the region with higher population reduces due the transport of excitation toward the outer regions (cf. for example, radial profiles at spatial position z = 1 mm). (iii) There are clear changes in axial direction, which arise both from application of collisional-radiative model and radiation transport effects. The differences are less pronounced for higher excitation energies.

Formally, the changes should appear for the species which are directly involved into radiation transport, i.e. $\mathrm{Ar}(1s_4)$ and $\mathrm{Ar}(1s_2)$. However, there are two major kinetic pathways which connect various excited species (levels between each other). The first pathway is the excitation in electron collisions, for example

$$\mathrm{Ar}(1s_4) + e \rightarrow \mathrm{Ar}(2p_{10}) + e \tag{7}$$

In such a way the changes in density distributions of $1s$ levels becomes „transported“ to $2p$ levels. However, this channel is weaker comparing with the second pathway. $\mathrm{Ar}(1s)$ levels are closely connected with each other via excitation processes in the electron collision and subsequent radiative deexcitation. An example of corresponding reaction pathway is as follows:

$$\mathrm{Ar}(1s_4) \xrightarrow{e} \mathrm{Ar}(2p_{10}) \xrightarrow{h\nu} \mathrm{Ar}(1s_5) \tag{8}$$

Therefore, the changes in population of resonance states lead to corresponding deviation in populations of all excited states. In the case of lowest excited states ($1s$ states) the differences arise up to seven orders of magnitude in the arc fringes. The broadening of the $2p$ states profiles is less pronounced in the central part of the arc, but achieve about two orders of magnitude in the arc fringes.

Inclusion of the full radiation transport in the equation system (model C) causes the spatial redistribution of $\mathrm{Ar}(1s)$ excited states densities. For higher excited states, like e.g. $2p$ and higher, the approach of effective lifetime can be applied.

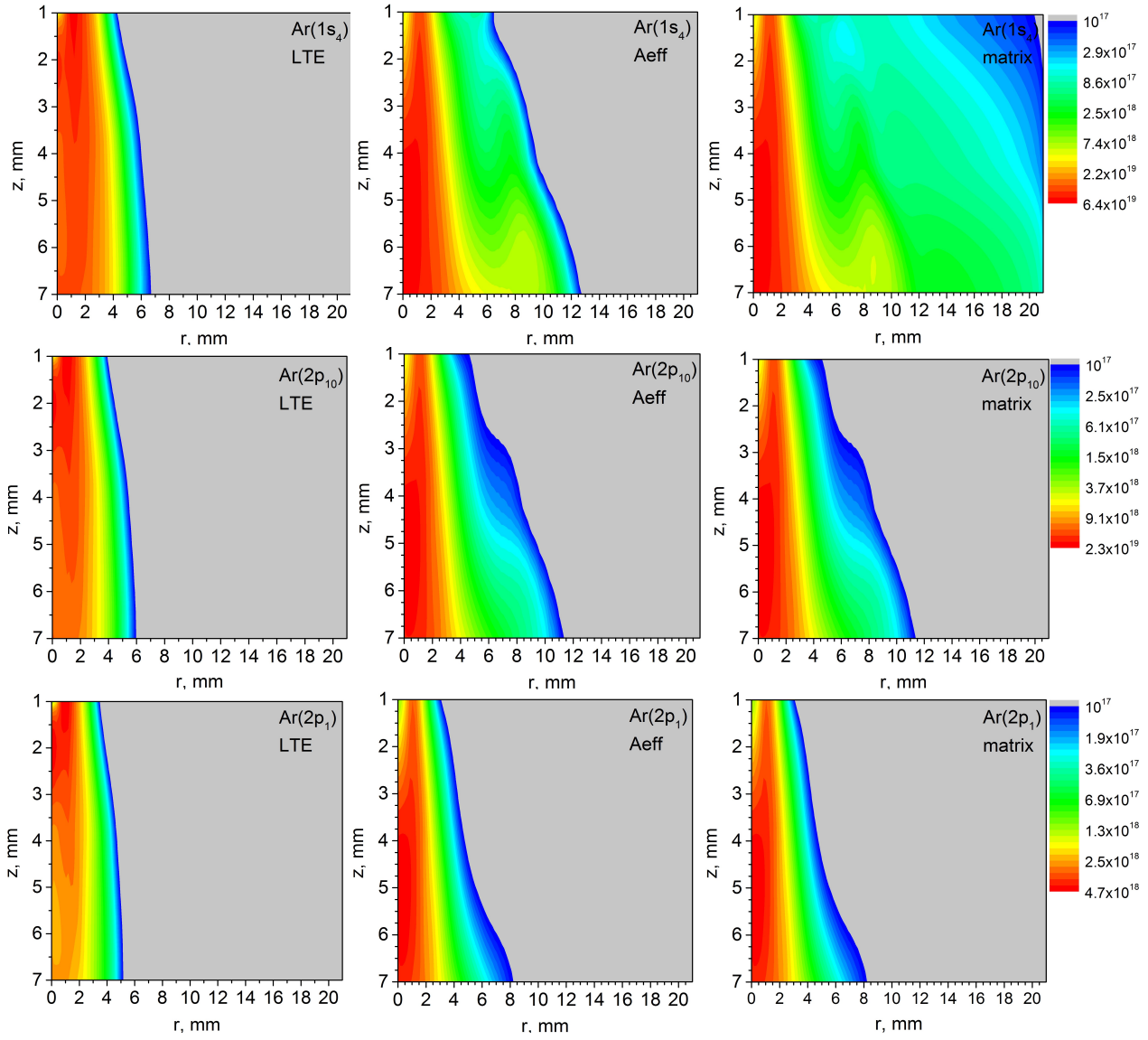

Figure 3. Spatial distributions of excited atom density (logarithmic scale, in m^{-3}) for different states predicted by model A (left row), model B (middle row) and model C (right row).

4. Conclusions

Resonance radiation trapping plays an important role in formation of spatial density profiles of excited atoms in a free-burning Ar arc. A noticeable growth of the $1s$ and lower lying $2p$ states population in the arc fringes takes place due to resonance radiation transport. These states are highly mixed due to collisional-radiative processes. For the higher excited levels which have a short lifetime and less connections to other states via excitation-de-excitation reactions this effect becomes less pronounced with increasing excitation energy of the level. Finally, the broadening of radial profiles due to the resonance radiation transport becomes negligible for high-lying excited states. Notice that the effect of profile broadening has a certain dependency on spatial distribution of absorption coefficient κ, which was not accounted for. Consideration of correct κ values can decrease the absolute values of excited species densities in the arc fringes [4].

References

[1] M. Baeva et al. Two-temperature chemically non-equilibrium modelling of transferred arcs. *Plasma Sources Sci. Technol.*, 21(5), 2012. doi:10.1088/0963-0252/21/5/055027.

[2] M. Baeva and D. Uhrlandt. Plasma chemistry in the free-burning ar arc. *J. Phys. D: Appl. Phys.*, 46(32), 2013. doi:10.1088/0022-3727/46/32/325202.

[3] M. Baeva. Thermal and chemical nonequilibrium effects in free-burning arcs. *Plasma Chem. Plasma Proc.*, 36(1):151–157, 2016. doi:10.1007/s11090-015-9650-9.

[4] Y. Golubovskii et al. Effects of traping of resonance radiation in free-burning ar arc. *J. Phys. D: Appl. Phys.*, 48(22), 2015. doi:10.1088/0022-3727/48/22/225203.

[5] L. M. Biberman. On the theory of the diffusion of resonance radiation. *Zh. Eksp. Teor. Fiz*, 17:417, 1947.

[6] T. Holstein. Imprisonment of resonance radiation in gases. *Phys. Rev.*, 72(12):1212–1233, 1947. doi:10.1103/PhysRev.72.1212.